CEA Comité Español de Automática

XLV JORNADAS AUTOMÁTICA MÁLAGA 2024

UNIVERSIDADE DA CORUÑA

Jornadas de Automática

Aproximación de tacto basada en fuerza para estimación de volumen

Castano-Amoros, J.[a,*], Trebuchon, K.[b], Gil, P.[a], Mezouar, Y.[b]

[a] *Universidad de Alicante, San Vicente del Raspeig, Alicante, Spain.*
[b] *Université Clermont Auvergne, Clermont-Ferrand, Auvergne, France.*

To cite this article:
Castano-Amoros, J., Trebuchon, K., Gil, P., Mezouar, Y. 2024. Force-based touch approach for volume estimation. Jornadas de Automática, 45. https://doi.org/10.17979/ja-cea.2024.45.10763

Resumen

Un agarre robótico óptimo no puede limitarse a la estimación de pose de agarre del objeto mediante visión. Se hace necesario el uso de sensores táctiles para conocer las propiedades físicas de los objetos que se agarran. En este trabajo, integramos dos sensores táctiles Contactile basados en la fuerza con una pinza ROBOTIQ 2F-140 y un robot UR5, para estimar el volumen de un recipiente lleno de agua utilizando redes neuronales Perceptrón Multicapa (MLP). Durante la experimentación entrenamos y evaluamos diferentes MLPs variando las fuerzas de entrada (Fx, Fy, Fz) en una tarea de regresión de volumen discreto en un rango de entre 0ml y 300ml. El enfoque preliminar propuesto se compara con un método algebraico basado en el diagrama del equilibrio de fuerzas, demostrando que nuestros resultados son más precisos, obteniendo un valor R^2 un 8 % superior en el peor de los casos, y del 30 % en el mejor.

Palabras clave: Percepción y detección, Robótica inteligente, Robots manipuladores, Tecnología Robótica

Force-based touch approach for volume estimation

Abstract

Optimal robotic grasping cannot be limited to the estimation of object grasping pose using vision-based methods. It is necessary to use tactile sensors to learn the physical properties of the objects that are to be grasped. In this work, we integrated two Contactile force-based tactile sensors with a 2F-140 ROBOTIQ gripper and a UR5 robot to estimate the volume of a water-filled container using Multilayer Perceptron (MLP) neural networks. During experimentation, we trained and evaluated different MLPs varying the input forces (Fx, Fy, Fz) in a task of discrete-volume regression in a range of between 0ml and 300ml. The preliminary proposed approach is compared with an algebraic method based on the diagram of the equilibrium of forces, proving that our results are more precise, obtaining a R^2 value of 8 % higher in the worst-case scenario, and of 30 % in the best.

Keywords: Perception and sensing, Intelligent Robotics, Robots manipulators, Robotics technology

1. Introduction and Related work

Traditionally, the research about robotic manipulation and tactile sensing has been focused on the detection of physical behaviors or events caused by undesired movements between the tactile sensors and the surface of the grasped objects, for example, the cases of contact (Zhang et al., 2019) or slippage (Castaño-Amorós and Gil, 2023) prediction, estimation of the grasping pose (Dikhale et al., 2022), etc.

However, another aspect that has not been explored as much is the knowledge of the dynamic properties of robotic grasping, such as when an object like a bottle contains liquid. This internal weight could provoke instability during the grasping of the object, leading to non-optimal control and manipulation, or even causing collisions or object falls in the worst case. It is, therefore, obvious that obtaining more knowledge about this type of dynamic properties (volume, viscosity, density, etc.) will help to improve the robot's skills applied to ma-

*Autor para correspondencia: julio.ca@ua.es

nipulation tasks. To do so, the use of tactile sensors is adequate because they can provide multi-modal data about physical phenomena caused during the object handling task.

The development of touch-based sensors has grown exponentially in recent years, resulting in a large number of different force and tactile sensors. In grasping, force sensors are usually installed on the wrist of the robot whereas tactile sensors are installed on the phalanges of a gripper or on a tool mounted on the effector. Both of them respond to the applied force and convert the value into a measurable magnitude. For example, the most common tactile sensors are electrical-based sensors, which employ capacitive technology, resistive, optical, etc. (Chi et al., 2018). Some of these sensors (Khamis et al., 2019) are capable of providing pressure values for a contact area while others only provide a representation of the contact without knowledge of the applied forces (Yuan et al., 2017), (Lambeta et al., 2020).

In this work, tactile sensors have been applied for the aforementioned purpose, which is to estimate the volume of a water-filled container like a bottle or jar. In recent works, other authors tried to solve similar tasks. For instance, in (Silva et al., 2019), the authors used 3D force sensors to estimate the weight of a cup filled with different volumes of sand by studying the diagram of applied forces during the grasping. In (Huang et al., 2022), the authors utilized the oscillations of the markers of a Gelsight optical sensor caused by the movement of a grasped bottle filled with liquid, to regress the liquid viscosity and height value using a Gaussian Process Regression model. Other examples are the works done in (Zhu et al., 2022) and (Chareyre et al., 2022), where they combined data from cameras and tactile sensors to estimate the volume of a liquid in a container using a multi-task learning approach, and they learned a policy to estimate general properties of an object using only pushing actions, respectively.

Our work differs from others in the literature in that we let neural networks learn the mapping between the input forces and object properties like the volume of the container, rather than studying the forces applied during the grasping task, and our preliminary results show that this is a more accurate way to approach the task. We also consider that force-based tactile sensors are more appropriate than optical-based tactile sensors for the task of volume estimation because it is easier to characterize the force from a reading that represents the magnitude than from an image contact as provided by an image-based tactile sensor. This is, it is easier and explainable to use force values in newtons (N) as input to a control algorithm than contact images that do not have a direct representation in N, as discussed in (Zapata-Impata et al., 2019b) and (Zapata-Impata et al., 2019a).

This paper is organized as follows: Section 2 describes the integration between the tactile sensors, our controller, and the rest of the hardware, Section 3 explains the calibration process that the sensor needs to keep the operating temperature and the force readings stable. In Section 4, the proposed task, the recorded data, and the utilized methods are explained in detail, while in Section 5 the results from the proposed methods are compared. Finally, Section 6 summarizes the results and future lines of work.

2. Software and Hardware Integration

This work revolves around the use of Contactile force sensors (Khamis et al., 2019) (see Figure 1).

They consist of an array of nine pillars in a 3x3 configuration. The center pillar is the tallest, and those in the corners are the shortest. The sensing tips are made of silicone, which behaves like a linear spring. This means that when grasping an object, the outermost pillars will slip more easily than the center pillar because the normal force applied to them is weaker. Besides, the main advantage of these sensors over others based on other technologies such as optics (i.e. DIGIT, GelSight, etc.) is that they are capable of estimating a force vector of the pressure exerted.

To make it applicable to robotic manipulation, we carry out a sensor integration process, which tackled two major issues: communication between the sensors and the existing robotic system, and assembling the sensors on the gripper.

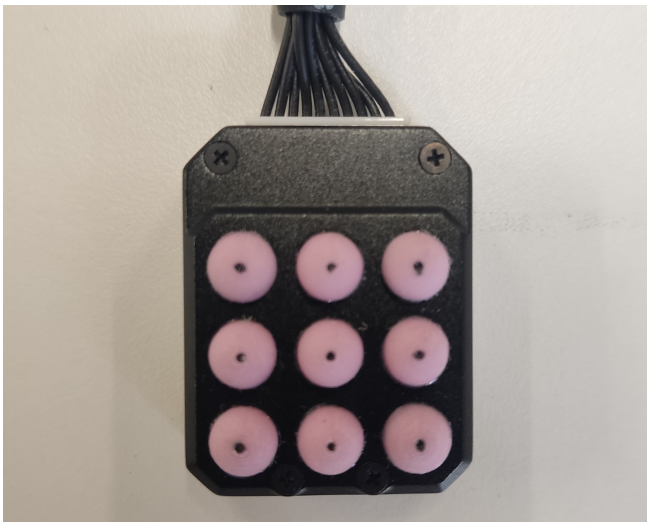

Figura 1: One of our Contactile sensors containing the 9 pillars in a 3x3 matrix configuration.

We use ROS (Robotic Operative System) to communicate the Contactile sensors with our Robotic Controller. The manufacturer of these sensors already provides the required ROS topics, messages, and services to carry out optimal data communication. Concretely, each Contactile sensor publishes force and displacement data from each of the nine pillars, and also the global values. In this work, only the global tridimensional force (Fx, Fy, Fz) from one sensor is utilized, which is calculated as described in Eq. 1.

$$Fx = \sum_{i=1}^{9} fx_i \qquad Fy = \sum_{i=1}^{9} fy_i \qquad Fz = \sum_{i=1}^{9} fz_i \quad (1)$$

where Fx, Fy, and Fz correspond to the global forces in axis x, y, and z, respectively, and fx_i, fy_i, and fz_i correspond to the forces in axis x, y, and z for each one of the nine pillars.

The following figure, Figure 2, shows a communication diagram between our Control Unit, the Contactile sensors, and the robotic gripper through ROS nodes.

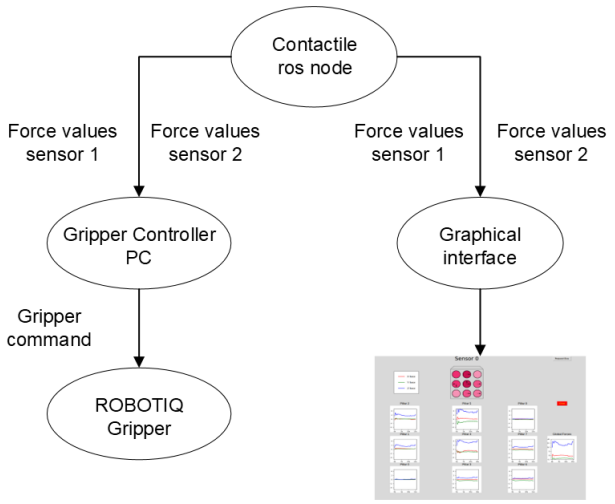

Figura 2: Data communication diagram between our PC, our Contactile sensors, and the ROBOTIQ 2F gripper.

In addition, the Contactile sensors already provide a graphical interface to show force values, nonetheless, this interface is only available for Windows OS and our Control Unit runs over Linux OS. In this work, we have, therefore, developed a custom graphical interface (see Figure 3) specific for Ubuntu OS using Tkinter and Matplotlib libraries, and the Python programming language.

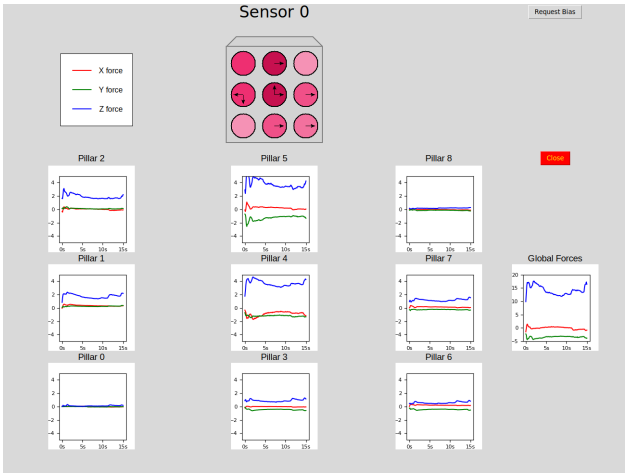

Figura 3: An example of the distribution of our interface when grasping the container. Note that the order of the plots of each pillar is organized as each circle in the layout.

Our interface shows a layout of each running Contactile sensor, which contains a 2D representation of each of the pillars, drawn as a circle. Each circle contains a color related to the applied force, on axis z, to the corresponding pillar in the real sensor. This color turns to a darker red when the applied force increases, and turns to a lighter pink when the applied force decreases. Negative forces on axis z are represented with a gray color, although they are not representative, as they are produced by noise in the sensors. Besides the intuitive visualization with colors of force data on axis z, we have also included arrows to indicate the direction and sense of the force data on axis x and y for each of the pillars. Moreover, a 2D plot containing force data (fx_i, fy_i, fz_i) is shown for each pillar, and another 2D plot which only contains global forces (Fx, Fy, Fz).

To assemble the two Contactile sensors with our ROBOTIQ_2F gripper, a 3D support was designed and 3D printed to fix each sensor to the robotic gripper. The design of the support and the printed piece are shown in Figure 4.

The support was designed to geometrically align the sensing zones of the Contactile sensors with the sensing zones of other tactile sensors available in our lab, to obtain multi-modal tactile feedback to use in future works. That way our 3D design for the Contactile sensors can be used independently or jointly without modifying the overall grasping geometry. So, after marking the center of the other tactile sensors, we took measurements with a caliper. From this, we determined that the support should have a 5.3mm-deep slot to accommodate the sensor while making sure the central pillar sticks out to the same height as the rest of the tactile sensors, and while ensuring proper protection against lateral impacts. However, because the Contactile's cable can't exit through the back of the mount without being excessively bent, we added a 30° slope to keep the cable as straight as possible along the fingers. We also included counterbores to the screw holes so that the screw heads don't interfere with the cable's movements during use.

With the sensors mounted on the gripper, the only remaining task was to find a way to put the controller unit on the robot arm. We opted for a two-part bracket that would be tightened around the circular portion of the last link of the robot, just below the end-effector. This positioning prevents relative movement between the gripper and the controller when rotating the end-effector, thus avoiding premature wear of the cables.

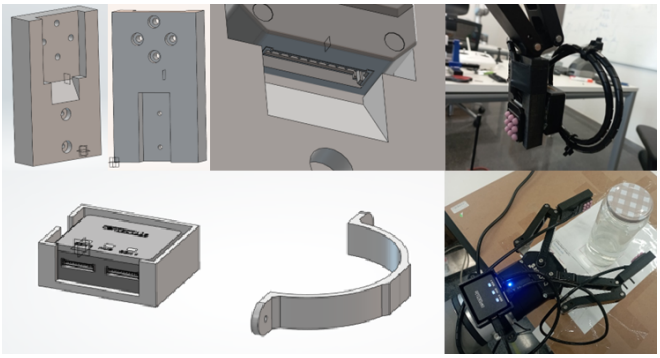

Figura 4: Design of case for Contactile sensor and mounting on 2F-140 ROBOTIQ gripper. (Top) Support to hold the sensor. (Bottom) Compartment and bracket to hold the controller. Link to download CAD files.

3. Sensor Calibration

Temperature plays a critical role in converting the contact signal reading into a pressure value. Prolonged use of the sensors will cause the electronics to overheat, reducing the reliability of the measurement. We could control the temperature range of the local ambient environment (air-conditioning system) to accomplish the tactile sensor works within a specified temperature range, but it would be very difficult to control the local temperature of the device and its circuits. This would

require the use of a heatsink but there is no physical space in the gripper. Other alternatives such as using liquid cooling or introducing insulating materials inside the sensor were not considered since it is a commercial sensor that would imply a loss of warranty. To reduce the cumulative measurement error caused by the heat build-up that occurs with the use, we have decided to automatically re-calibrate the sensor at regular intervals of time. Overheating causes an increase in the measurement provided by the sensor, therefore it is necessary to determine the maximum allowable time after which the temperature can cause inaccuracy in the pressure measurement, to reset the value to zero by calling the manufacturer's driver.

First, we placed one sensor on a flat, horizontal surface with the pillars pointing vertically upwards. Then we turned it on, calibrated it using the bias function provided by the manufacturer to set the zero, recorded five seconds of the output, and let it heat up for thirty minutes without putting any weight on it. During that time, a five-second sample was recorded in a rosbag every five minutes, resulting in seven measures throughout the experiment. We repeated the same process once, but during the last test, a $500g$ object was placed on the sensor before recording a rosbag, and then removed. This was meant to see if measured weight had an impact on the drift. Figure 5 shows the measurements and deviation from the reference weight in both experiments.

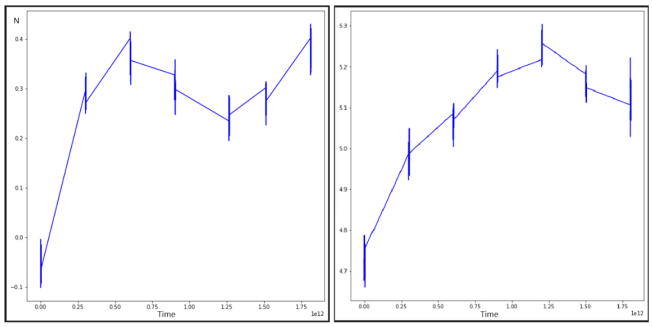

Figura 5: (Left) Measurements without any weight applied. (Right) Measurements with a weight of $500g$.

Once the data was recorded, we plotted the values and tried fitting a mathematical model to the curves. This model should be able to fit other curves representing intermediate weights between 0 and $500g$. The idea was to find a model that generalize the behavior independently of the chosen weight curve. Polynomial regression gave a good approximation of a given curve. For the best cases, it was around 0.88 but it only returned an R^2 of around 0.6 on the other tests. It also seems that additional weight increases the output drift. When left alone, the reading of sensor increased by $0.3N$ in $30min$, but when the object was weighed, the error increased to $0.5N$.

In the end, real-time drift correction depends on too many factors to be reliable. We would advise either calibrating the sensor before each measurement or calibrating every five minutes for better results.

4. Data, methods and learning

Before describing our dataset, it is important to clarify what the task proposed in this work is: to estimate the volume in milliliters (ml) of a water-filled container grasped and held by a robot, from the force values obtained by a Contactile force sensor. Figure 6 shows an example of the robot grasping the container, and a diagram with the corresponding forces.

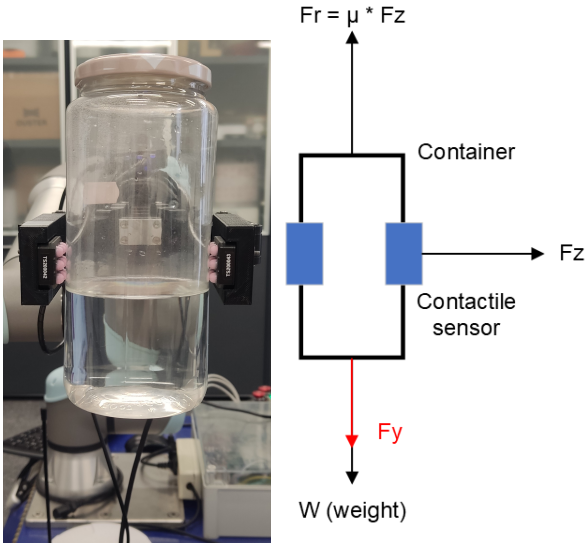

Figura 6: (Left) Container filled with 250ml of water grasped by our UR5 robot using the 2F-140 ROBOTIQ gripper and the Contactile sensors. (Right) Diagram of applied forces during grasping.

Note that F_y and W would be equivalent in the case of a static setup, in which the gripper is performing a firm grasp. However, in this work, the setup used to collect the data is dynamic, not static, so we cannot ensure a firm grasp. We, therefore, need to consider F_y and W as different variables.

To record our dataset, a fixed trajectory is planned for the robot, which consists of grasping the container, lifting it $10cm$, and placing it on the table again, while the Contactile sensors record the force values. Note that only the forces generated when the container is not in contact with the table are considered. This process is repeated 14 times per volume, i.e. $\{0, 50, 100, 150, 200, 250, 300\}ml$ of water. Our dataset therefore consists of 98 lifts that correspond to a total of 201248 force values, approximately an average of 2053 force values per lift.

Instead of splitting our dataset in a single train, validation, and test configuration, a 5-fold cross-validation technique is applied to generate 5 random sub-datasets ($d1$, $d2$, $d3$, $d4$, and $d5$) with 10 random lifts of each volume for the training set (70 lifts in total), and the remaining 4 lifts of each volume for the test set (28 lifts in total).

In this work, we pretend to solve the proposed task utilizing 2 different methods to evaluate their performance later.

The first method consists of training an MLP neural network to estimate a discrete volume $\{0, 50, 100, 150, 200, 250, 300\}ml$ of the water-filled container. The MLP neural network consists of a single hidden layer with 2 neurons. Note that deeper networks do not improve the performance in this task. Figure 7 shows a simplified diagram of our MLP and the corresponding mathematical equations to calculate the output ($\hat{y}$) are shown in Eq. 2.

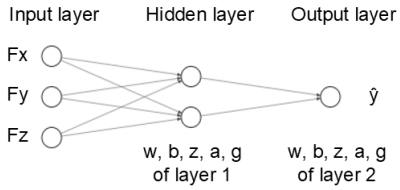

Figura 7: Simplified diagram of the MLP neural network with 2 neurons in the hidden layer.

$$
\begin{aligned}
z^{[1]} &= w^{[1]} \cdot x + b^{[1]} \\
a^{[1]} &= g^{[1]}(z^{[1]}) \\
z^{[2]} &= w^{[2]} \cdot a^{[1]} + b^{[2]} \\
a^{[2]} &= \hat{y} = g^{[2]}(z^{[2]})
\end{aligned}
\tag{2}
$$

where x are the input force values, $w^{[1]}$, $b^{[1]}$, $w^{[2]}$, and $b^{[2]}$ correspond to the model weights and biases from layers 1 and 2, $z^{[1]}$ and $z^{[2]}$ represent the lineal output before applying the activation function from layers 1 and 2, $a^{[1]}$ and $a^{[2]}$ correspond to the calculated activation values from layers 1 and 2, respectively. Note that $g^{[1]}$ is a Rectified Linear Unit (ReLU) activation function, while $g^{[2]}$ is a linear activation function that returns a continuous estimation of the volume.

Besides the MLP, an algebraic method is implemented to estimate the weight of the water-filled container from the force values. This method is useful to compare the results of our MLP with a baseline model. The formula that defines this baseline method is shown in Eq. 3.

$$
est\_vol = 1000 \times \frac{Fy + \mu \times Fz}{G} - m\_cont \tag{3}
$$

where est_vol is the estimated volume in ml, Fy is the force reading from the Contactile sensor on axis y (see Figure 6), μ is the friction coefficient of the container, Fz is the grasping force obtained by the Contactile sensor on axis z (see Figure 6), G is the gravity ($9.81 m/s^2$), and m_cont is the weight of the empty container ($56g$).

Regarding the learning phase of both methods, on the one hand, the MLP needs to learn the optimal parameters $w^{[1]}$, $b^{[1]}$, $w^{[2]}$, and $b^{[2]}$ to minimize its cost function. Hyperparameter optimization was performed using the grid search technique. On the other hand, the second method needs to estimate the friction coefficient of the plastic (PET) container, which is selected based on other previous studies. The R^2 metric is used to evaluate the performance of both methods (see Eq. 4).

$$
R^2 = 1 - \frac{\sum_{i=1}^{m}(y\_true - \hat{y})^2}{\sum_{i=1}^{m}(y\_true - \overline{y\_true})^2} \tag{4}
$$

where m is the total number of samples, y_true is the ground truth volume, $\hat{y}$ is the estimated volume, and $\overline{y\_true}$ is the mean of y_true for the m samples. Note that the highest value of R^2 metric is 1.0.

Concerning the learning phase of the proposed MLP, the following hyperparameters were set through a grid search: one hidden layer with two neurons, ReLU activation for the hidden layer, Adam optimization solver, $L2$ regularization term of 0.0001, batch size of 200 samples, learning rate equal to 0.001, and a tolerance error to stop the training earlier of 0.0001 that defines the number of training epochs.

To estimate the friction coefficient (μ) of the container, we calculated Eq. 3 with 200 μ-values ranging from 0.1 to 0.4 for the 5-fold training sets ($d1\_train$, $d2\_train$, $d3\_train$, $d4\_train$, and $d5\_train$) as can be seen in Figure 8. Thus, we obtained a μ-value that maximizes the R^2 metric for each training fold, and we estimated the optimal μ-value (0.268) as the average of these μ-values. This average μ is used on the test data.

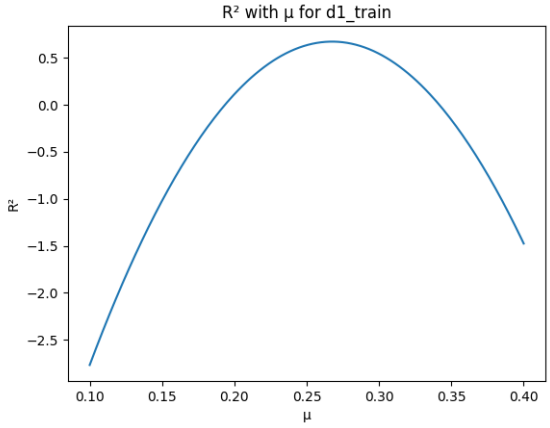

Figura 8: Curve R^2-μ corresponding to $d1\_train$.

5. Experiments, analysis and results

The most relevant forces involved in a vertical displacement of a planar grasping are the force readings on the axis y and z (see Figure 6). The force reading on axis x is almost negligible.

To evaluate the influence of the forces on the different axes for the task of volume estimation, the MLP was trained with different combinations of forces as input: i) $\{Fx, Fy, Fz\}$, ii) $\{Fy, Fz\}$, iii) Fy, and iv) Fz. The MLP has been trained once for each of the four input modalities and each training fold, and later, it has been evaluated on each test fold ($d1\_test$, $d2\_test$, $d3\_test$, $d4\_test$, and $d5\_test$). Thus, five R^2 values have been calculated for each input modality. The following bar plot, Figure 9, shows the mean R^2 value and standard deviation of the 5 test folds for each input modality.

The results shown in Figure 9 are compared with the results obtained using the baseline method described in Eq. 3 in Table 1. These results show that the MLP learned to map the input forces to the volume of the container in a more precise way when compared to the study of the forces applied during the grasping. This can happen because the MLP performs a best approximation of the mathematical function without the knowledge of the physical properties of the grasping task, which may not be taken into account in Eq. 3. Another negative factor is the fact that the estimation of the friction coefficient μ may not be very precise, since it has a different value for each object and material. Table 2 shows the results of the best version of our MLP, which is the one using Fy and Fz as input forces, when testing with the volume quantities defined in our dataset. We have also tested with other intermediate volumes, which were not considered during the training phase,

seeking to prove how the model generalizes. Although the estimations corresponding to the intermediate volumes are less accurate, they are still quite promising, which proves that our approach is able to generalize to other volumes, e.g. for a container with 75ml and 125ml, the method estimates 73.62ml and 134.57ml, respectively.

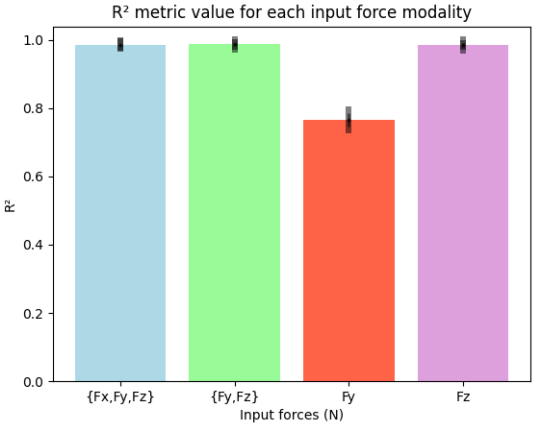

Figura 9: Results in terms of R^2 metric of the MLP trainings with different input forces.

Tabla 1: Results comparison between MLP methods shown in Figure 7 and baseline method *est_vol* from Eq. 3.

Method	R^2
$\{Fx, Fy, Fz\}$	0.9852 ± 0.0011
$\{Fy, Fz\}$	0.9862 ± 0.0036
Fy	0.7651 ± 0.0195
Fz	0.9842 ± 0.0049
est_vol (baseline)	0.6817 ± 0.0122

Tabla 2: Volume estimation using the best approach based on MLP $\{Fy, Fz\}$.

$y\_true(ml)$	$\hat{y}(ml)$
0	19.62
50	56.74
100	105.04
150	150.32
200	190.75
250	239.07
300	313.06

6. Conclusiones

In this work, we have developed an initial implementation of a tactile-based robotic system to estimate the volume of a water-filled container by mapping input force values to milliliters using MLP neural networks. We obtained preliminary results that prove that the force Fz is the more relevant force involved in the grasping and vertical lift of the container obtaining a R^2 metric value around 0.98, being the forces Fy and Fx less important for this task. This approach performs better for this task compared with other approaches such as the analysis of the equilibrium forces applied during the grasping. Nonetheless, our system is still in the early stages of development. We are therefore working on a fully continuous regression method instead of our discrete version as well as comparing it with other state-of-the-art methods. We also plan to extend our method to estimate the volume of liquids other than water, such as oil or detergent.

Acknowledgement

This work was supported in part by Spanish Government through Project PID2021-122685OB-I00 and in part by Interreg-VI Sudoe and European Regional Development Fund through the REMAIN project (S1/1.1/E0111) and by the University of Alicante under Grant UAFPU21-26.

Referencias

Castaño-Amorós, J., Gil, P., 2023. Measuring object rotation via visuo-tactile segmentation of grasping region. IEEE Robotics and Automation Letters 8 (8), 4537–4544.
DOI: 10.1109/LRA.2023.3285471

Chareyre, M., Fournier, P., Moras, J., Mezouar, Y., Bourinet, J.-M., 2022. Towards generic object property estimation using unsupervised reinforcement learning. In: Int. Conf. on Intelligent Robots and Systems (IROS). Workshop on Mobile Manipulation and Embodied Intelligence: Challenges and Opportunities. Kyoto, Japan.
DOI: hal.science/hal-03927900

Chi, C., Sun, X., Xue, N., Li, T., Liu, C., 2018. Recent progress in technologies for tactile sensors. Sensors 18 (4).
DOI: 10.3390/s18040948

Dikhale, S., Patel, K., Dhingra, D., Naramura, I., Hayashi, A., Iba, S., Jamali, N., 2022. Visuotactile 6d pose estimation of an in-hand object using vision and tactile sensor data. IEEE Robotics and Automation Letters 7 (2), 2148–2155.
DOI: 10.1109/LRA.2022.3143289

Huang, H.-J., Guo, X., Yuan, W., 2022. Understanding dynamic tactile sensing for liquid property estimation. In: Robotics: Science and Systems (RSS). IFRR, New York, USA.
DOI: 10.48550/arXiv.2205.08771

Khamis, H., Xia, B., Redmond, S. J., 2019. A novel optical 3d force and displacement sensor – towards instrumenting the papillarray tactile sensor. Sensors and Actuators A: Physical 291, 174–187.
DOI: 10.1016/j.sna.2019.03.051

Lambeta, M., Chou, P.-W., Tian, S., Yang, B., Maloon, B., Most, V. R., Stroud, D., Santos, R., Byagowi, A., Kammerer, G., Jayaraman, D., Calandra, R., 2020. Digit: A novel design for a low-cost compact high-resolution tactile sensor with application to in-hand manipulation. IEEE Robotics and Automation Letters 5 (3), 3838–3845.
DOI: 10.1109/LRA.2020.2977257

Silva, A., Brites, M., Paulino, T., Moreno, P., 2019. Estimation of lightweight object's mass by a humanoid robot during a precision grip with soft tactile sensors. In: Int. Conf. on Robotic Computing (IRC). IEEE, pp. 344–348.
DOI: 10.1109/IRC.2019.00062

Yuan, W., Dong, S., Adelson, E. H., 2017. Gelsight: High-resolution robot tactile sensors for estimating geometry and force. Sensors 17 (12).
DOI: 10.3390/s17122762

Zapata-Impata, B. S., Gil, P., Torres, F., 2019a. Learning spatio temporal tactile features with a convlstm for the direction of slip detection. Sensors 19 (3).
DOI: 10.3390/s19030523

Zapata-Impata, B. S., Gil, P., Torres, F., 2019b. Tactile-driven grasp stability and slip prediction. Robotics 8 (4).
DOI: 10.3390/robotics8040085

Zhang, Y., Yuan, W., Kan, Z., Wang, M. Y., 2019. Towards learning to detect and predict contact events on vision-based tactile sensors. In: 3rd. Conf. on Robot Learning (CoRL). IFRR, Osaka, Japan.
DOI: 10.48550/arXiv.1910.03973

Zhu, F., Jia, R., Yang, L., Yan, Y., Wang, Z., Pan, J., Wang, W., 2022. Visual-tactile sensing for real-time liquid volume estimation in grasping. In: Int. Conf. on Intelligent Robots and Systems (IROS). IEEE/RSJ, Kyoto, Japan, pp. 12542–12549.
DOI: 10.1109/IROS47612.2022.9981153